ewec 2008 BRUSSELS
Europe's premier wind energy event

A new urban wind turbine blade design using a pressure-load inverse method

J. C. C. Henriques*
IDMEC, Instituto Superior Técnico
Technical University of Lisbon
Av. Rovisco Pais
1049-001 Lisboa, Portugal
joaochenriques@ist.utl.pt

F. Marques da Silva
LNEC - Laboratório Nacional
de Engenharia Civil
Av. Brasil, 101
1700-066 Lisboa, Portugal
fms@lnec.pt

A. I. Estanqueiro
INETI - Instituto Nacional de Engenharia,
Tecnologia e Inovação
Estrada do Paço do Lumiar
1649-038 Lisboa, Portugal
ana.estanqueiro@ineti.pt

L. M. C. Gato
IDMEC, Instituto Superior Técnico
Technical University of Lisbon
Av. Rovisco Pais
1049-001 Lisboa, Portugal
luis.gato@ist.utl.pt

Abstract

This paper presents the design methodology of a new wind turbine blade section that achieves high performance in urban environment by increasing the maximum lift. For this purpose, a turbomachine blade rows inverse design method was applied to obtain a new wind turbine blade section with constant pressure-load along the chord, at the design inlet angle. In comparison with conventional blade designs, the new blade section has increased maximum lift, reduced leading edge suction peak and controlled soft-stall behaviour, due to the strength reduction of the adverse pressure gradient on the blade suction surface. Wind tunnel experimental results confirmed the computational results.

Keywords: Blade section design, inverse method, prescribed blade load.

1 Introduction

Within urban environment, where the average mean wind speed is quite lower than in open rural or mountainous areas, it is of major relevance to have wind turbines with low cut-in speed, in order to increase the annual energy production and the overall contribution of this micro-generation renewable energy technology. For fixed pitch turbines, this requires blade sections with the highest possible lift. Although the overall performance of a wind rotor turbine is influenced by three-dimensional and unsteady effects, substancial gains can be achieved by a better design of the blade sections [1].

There are two distinct strategies for the design of turbomachine blade sections: the direct and the inverse methods. The first, giving origin to the so-called analysis or direct methods, uses a "cut-and-try" approach where the results are validated experimentaly or with the help of analysis codes. This procedure is usually slow, cumbersome and relies heavily in the experience of the designer. Opposite to this type of methods, the so-called inverse or indirect methods aim to calculate the blade geometry that provides certain conditions for the flow specified as initial data for the problem. Three major trends have been developed for the solution of the inverse problem: optimization techniques, pure inverse formulation methods and iterative use of analysis (or direct) codes. When using optimization techniques [2], the blade sec-

*Corresponding author. Tel: +351 21 841 7411, Fax: +351 21 841 7398

tion is described in terms of some parameters and a search is initiated in the design range, looking for the set of parameters that give the computed flow features as close as possible to the ones specified, or that lead to an optimum regarding some flow field conditions. Pure inverse methods [3–5] determine directly the geometry of the blade section that will achieve certain desired flow conditions. This is done by means of a problem formulation that makes immediate use of the information supplied by these desired flow conditions, for example, by using the imposed flow conditions as boundary conditions. For a more complete review of the current blade design methods see [6] and the references therein.

This paper presents the results of the application of the turbomachine blade rows inverse method developed by Borges *et al.* [7] to the design of a new wind turbine blade section that reaches an almost constant blade pressure-load along the chord. Unlike the pure inverse methods - which determine directly the blade geometry that achieves the specified desired flow conditions by means of a problem formulation making immediate use of the information supplied by these desired flow conditions - the current formulation is based on the iterative use of analysis codes. The design method uses as input the imposition of the mass averaged tangential velocity distribution along the chord (which is directly related with the blade load) and the desired blade section thickness. As a result, we imposed the blade load, defined as the pressure difference between both sides of the blade section, by modifying the camber. Another important feature of the method is that by imposing the blade load we are also prescribing the blade section lift at the design conditions. Consequently, the final result is weakly dependent of the thickness distribution for streamlined shapes with thickness-to-chord ratios within the normal range for wind turbine applications.

The current approach starts by assuming an initial geometry and calculates the flow field caused by it. The differences between the calculated flow field and the desired one are used to modify the original geometry. Afterwards, a new direct analysis of the flow field is made and a new iteration loop is entered. This iterative process is repeated until convergence is obtained. The code presently used in the direct analysis is a fast panel method for blade cascades [8].

Kamoun *et al.* [9] have used a related method that imposes circulation instead of the blade load. The current design method imposes indirectly the circulation by prescribing the pressure difference between both sides of the blades and hence the lift. By enforcing the blade load there is less control of the pressure distribution but the method is less prone to impossible solutions.

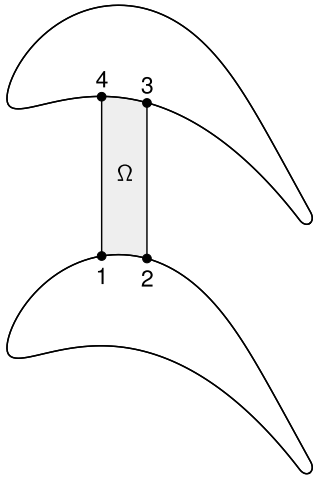

Figure 1: Typical control volume used for tangential momentum balance in a cascade of blades.

The aerodynamic characteristics of the designed blade as an isolated airfoil were computed with the well-know XFoil code [10] and the results were validated against the experimental data obtained in the LNEC wind tunnel.

2 Blade design

2.1 Design method

The design method used in the present paper combines a fast direct method based on a cascade panel method with a blade camber-line modification algorithm, in order to impose a prescribed blade load along the chord. The design condition is the mean momentum along the tangential direction, $\overline{M}_y$, defined as a function of the axial chord position. Let us consider the momentum balance along the tangential direction, y, in steady-state

$$\int_{\partial\Omega} (\varrho W_y \, \mathbf{W} \cdot \mathbf{n} + p n_y) \, \mathrm{d}s = 0, \tag{1}$$

where $\mathbf{n} = (n_x, n_y)$ is the outward unitary normal to the boundary, $\partial\Omega$. Applying this equation to the control volume depicted in Figure 1 gives

$$\int_{23} \varrho W_y W_x \, \mathrm{d}s - \int_{41} \varrho W_y W_x \, \mathrm{d}s + \int_{34} p \, \mathrm{d}x - \int_{12} p \, \mathrm{d}x = 0, \tag{2}$$

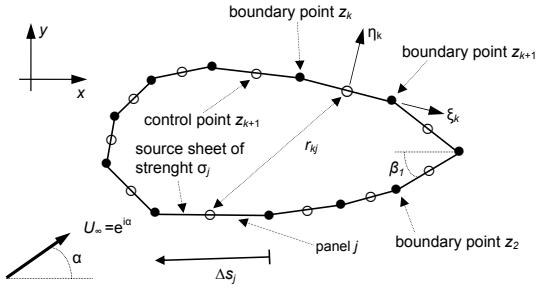

Figure 2: Surface panel distribution.

noting that $dx = n_y ds$ and $\mathbf{W}\cdot\mathbf{n} = 0$ on the blade surface. Taking a small Δx, we write

$$\int_{23} \varrho W_y W_x \, ds - \int_{41} \varrho W_y W_x \, ds = -\left(p_{ss} - p_{ps}\right) \Delta x. \tag{3}$$

Knowing that the mass flow is constant through the cascade of blades

$$\dot{m} = \int_{23} \varrho W_x \, ds = \int_{41} \varrho W_x \, ds \tag{4}$$

and making $\Delta x \to 0$, we get

$$\frac{d}{dx}\left(\frac{\int_{y_{ss}}^{y_{ps}} \varrho W_y W_x \, ds}{\dot{m}}\right) = -\frac{\Delta p}{\dot{m}}, \tag{5}$$

where $\Delta p = p_{ss} - p_{ps}$. Defining

$$\overline{M}_y = \frac{\int_{y_{ss}}^{y_{ps}} \varrho W_y W_x \, ds}{\dot{m}}, \tag{6}$$

we finally obtain

$$-\frac{\Delta p}{\dot{m}} = \frac{d\overline{M}_y}{dx}. \tag{7}$$

Relating the blade camber-line angle with the angle of the mean tangential velocity, the iterative modification of the mean line based on the specified blade load, (*sp*), is calculated from

$$\tan\theta^{n+1} = \tan\theta^n + \omega\left(\overline{M}_y^{\mathrm{sp}} - \overline{M}_y^n\right), \tag{8}$$

where ω is a relaxation factor, usually taken as $\omega = 0.5$, and n is the iteration number. After the mean line tangent being known, one can evaluate the mean line by solving the differential equation

$$\frac{dy_{\mathrm{cl}}}{dx} = \tan\theta. \tag{9}$$

To close the problem, it is necessary to define the blade thickness distribution and to prescribe the blade load along the axial chord, $\overline{M}_y^{\mathrm{sp}}$. The blade geometry is evaluated distributing the thickness along the normal direction to the mean line as done for the NACA four digit airfoils [11].

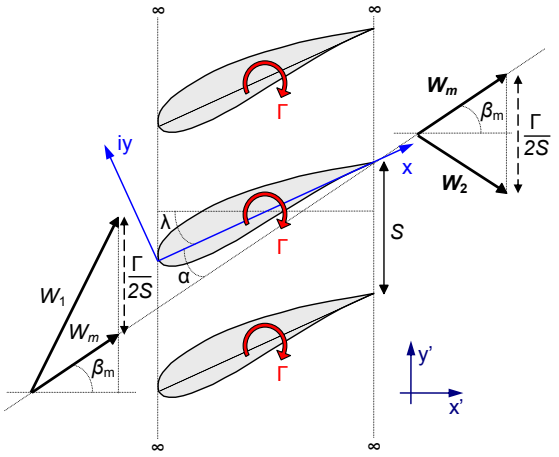

Figure 3: Vector diagram showing inlet and outlet velocities and angles.

2.2 Panel method

In many engineering applications the fluid flow around an aerofoil can be closely approximated as two-dimensional and incompressible. Making further assumptions and considering irrotational flow, it can be shown that the equations of motion are reduced to the simple Laplace equation (see, e.g. [12]). The linearity of Laplace equation is used in the theory of the panel method to decompose the flow around an aerofoil into two basic flows: the first is a non-lifting flow resulting from an uniform stream; the other is a pure circulatory flow that is superposed to the non-lifting flow, to satisfy the Kutta condition. The panel method has become a standard aerodynamic tool for the numerical solution of low-speed flows, since the late 1960s. However, various formulations of the panel method have been proposed, differing essentially in the way they implement these basic flows.

2.2.1 Isolated Aerofoil

In the present approach, we follow the methodology described by [13], which allows the calculation of cusped trailing edges. The aerofoil contour and its mean line are divided, respectively, in small flat N and M segments (panels) and then sources or vortexes are distributed in each panel to obtain the combined lifting flow. The non-lifting flow is simulated as a combination of a source sheet distribution of constant strength σ_j at each surface panel j, and an uniform stream at an incidence angle α, Figure 2. The complex velocity at a control point k is obtained adding the complex velocities evaluated, respectively, for the source

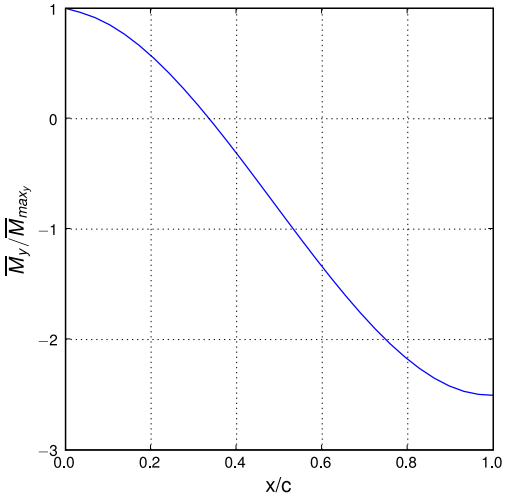

Figure 4: Prescribe blade load along the axial chord, $\overline{M}_y$.

Figure 5: The TURBan 10/193 blade section.

sheets [14],

$$w_k = -\frac{\mathrm{i}}{2}\sigma_k + \sum_{\substack{j=1 \\ j\neq k}}^{N} Q_{kj}\sigma_j, \tag{10}$$

and the onset uniform stream of unitary velocity,

$$w_k^{\infty} = \mathrm{e}^{(-\alpha+\beta_k)\mathrm{i}}. \tag{11}$$

Here β_k is the angle of the panel k with respect to the real axis x, Figure 2. For a single aerofoil, the induction coefficient Q_{kj} is given by [14]

$$Q_{kj} = \frac{\mathrm{e}^{(\beta_k-\beta_j)}}{2\pi} \ln \frac{z_k - c_{j_1}}{z_k - c_{j_2}}. \tag{12}$$

In Eq. (12) z_k is a complex variable representing the coordinates of the control point k and c_{j_1}, c_{j_2} are the values of the end points of panel j, in the local coordinate system $(\xi, \mathrm{i}\eta)$ shown in Figure 2. The imposition of the boundary condition of zero normal velocity at the body surface for the non-lifting flow, at $k = 1, \ldots, N$ control

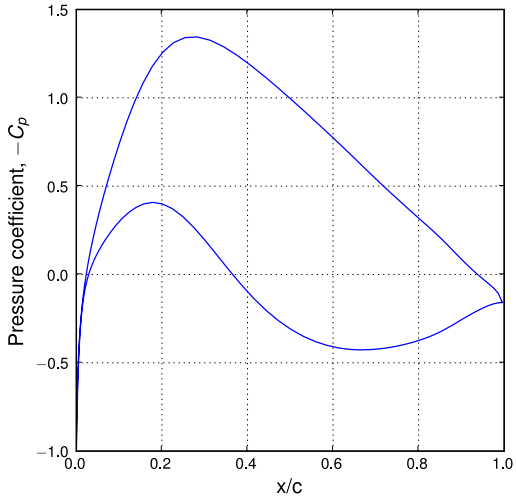

Figure 6: Pressure coefficient for the TURBan 10/193 blade section at the design conditions.

points, results in a simple linear system of N equations,

$$\mathrm{imag}(w_k) + \mathrm{imag}(w_k^{\infty}) = 0, \tag{13}$$

which can be solved for σ_j. The circulatory flow is obtained combining vortex sheets of constant strength at the mean line and source sheets in the surface panels, as for the non-lifting flow. Knowing that the overall circulation distribution in the aerofoil is arbitrary, as shown in [15], we will follow Eça [13] recommendation and use an overall hyperbolic variation that reaches zero at the trailing edge, as physically required,

$$\gamma_l = \gamma^0 s_l^{0.4}, \tag{14}$$

where γ_l is the strength of the vortex sheet in panel l of the mean line, s_l is the mean line length measured from the trailing edge to control point l, and γ^0 is such that the Kutta condition is satisfied. The total circulation around the aerofoil Γ is then obtained integrating Eq. (14) along the aerofoil mean line, from the leading edge to the trailing edge. Taking into account the simple relationship between the complex velocity induced by a vortex sheet (w_v) and a source sheet (w_s) of equal geometry and unitary strength, $w_v(z) = \mathrm{i}w_s(z)$, the velocity induced by the M vortex sheets in the k panel, per unit of γ^0, can then be written as

$$w_k^* = \sum_{l=1}^{M} \mathrm{i}Q_{kl}s_l^{0.4}, \tag{15}$$

where Q_{kl} is given by Eq. (12). The source strength σ_j^c required to satisfy the boundary

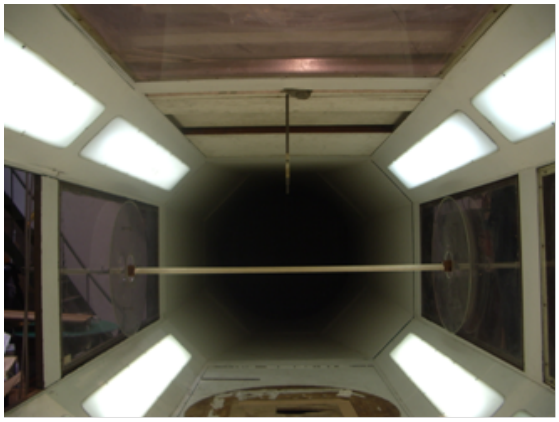

(a)

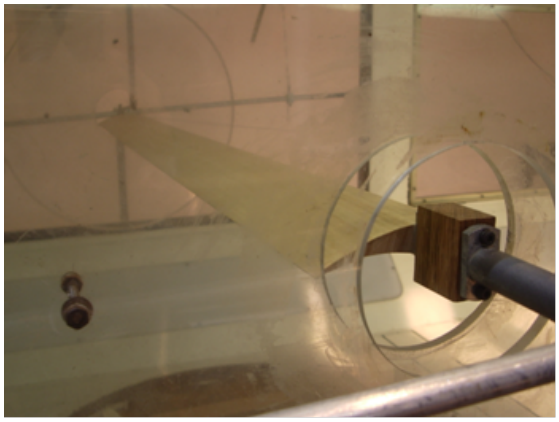

(b)

Figure 7: View of the LNEC wind tunnel (a) and the respective testing section (b).

condition of zero normal velocity at the body surface can be calculated from

$$\text{imag}(w_k^c) + \text{imag}(w_k^*) = 0, \tag{16}$$

where w_k^c is obtained introducing σ^c in Eq. (10). To impose the Kutta condition, we specify equal velocity (pressure) at the two control points adjacent to the trailing edge [15], from which we finally obtain the required constant value

$$\gamma^0 = \frac{\text{real}(w_1^\infty + w_N^\infty + w_1 + w_N)}{\text{real}(w_1^* + w_N^* + w_1^c + w_N^c)}. \tag{17}$$

2.2.2 Cascade of blades

For a blade cascade we adopt the global coordinate system $(x, \mathrm{i}y)$ shown in Figure 3. Using the same panel discretization in all the blades, we find $N + M$ rows of an infinite number of similar panels set with a pitch S along straight lines normal to the cascade axis. Instead of Eq. (12), derived for a single aerofoil, the induction coefficient for a blade cascade,

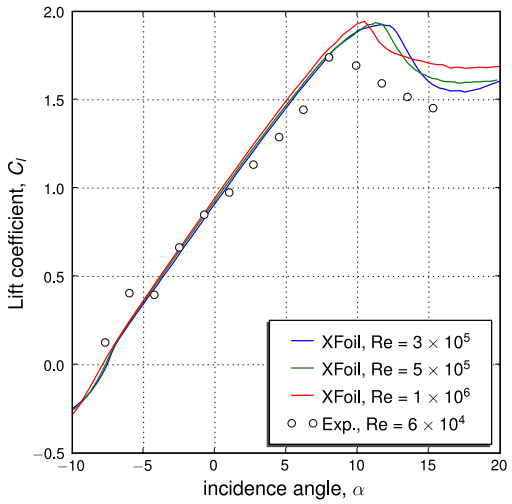

Figure 8: Lift coefficient as function of the incidence angle for the TURBan 10/193 blade section.

Figure 3, is [14]

$$Q_{kj} = \frac{\mathrm{e}^{\mathrm{i}(\beta_k - \beta_j)}}{2\pi} \ln \frac{\sinh\left(\frac{\pi}{S}\left(z_k - c_{j_1}\right)\right)}{\sinh\left(\frac{\pi}{S}\left(z_k - c_{j_2}\right)\right)}. \tag{18}$$

It can be shown that the coefficient of self induction given by Eq. (18) at $(\xi, \mathrm{i}\eta) = (0, +0i)$ is the same as that obtained for the isolated aerofoil (Eq. (12)), i.e. $Q_{kk} = -\mathrm{i}/2$. Therefore, cascade calculations can be performed along the same lines as described in Section 2.1 for the isolated aerofoil, simply replacing Eq. (12) by Eq. (18). This is the main advantage of using complex variables in the calculations. Having determined the blade circulation, the inlet and the outlet velocities (Figure 3) are easily computed from

$$\begin{aligned} w_1 &= \mathrm{e}^{\mathrm{i}\beta_m} + \frac{\mathrm{i}\Gamma}{2S}, \\ w_2 &= \mathrm{e}^{\mathrm{i}\beta_m} - \frac{\mathrm{i}\Gamma}{2S}. \end{aligned} \tag{19}$$

In addition, the inlet and outlet flow angles are given by

$$\begin{aligned} \beta_1 &= \arg(w_1), \\ \beta_2 &= \arg(w_2). \end{aligned} \tag{20}$$

2.3 Numerical results

The main goal of the current blade design method is to maximize the energy extraction at low wind speeds, a typical characteristic of urban environment. To achieve this goal, a blade section was designed with high-lift using the

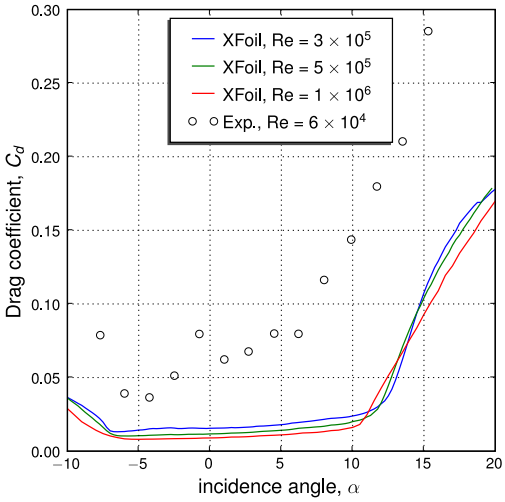

Figure 9: Drag coefficient as function of the incidence angle for the TURBan 10/193 blade section.

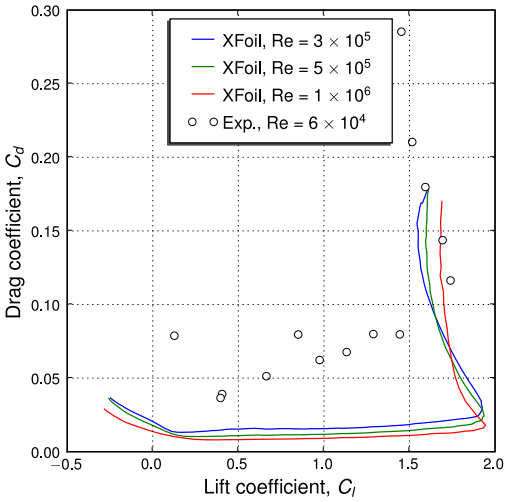

Figure 10: Polar of the TURBan 10/193 blade section.

method described in section 2.1. A linear distribution of the blade pressure-load was used for most of the axial chord and the load was smoothly reduced to zero at the trailing edge region, Figure 4. The blade was designed for a pitch-to-chord ratio of 1.72 and an inlet angle of β_1 = 4.0°. We note that it is necessary to iterate the incidence angle, α, in order to get the desired inlet angle because this angle is a function of the blade lift, which dependes on the blade camber. The maximum thickness of the current section is 17% at 26% of the chord.

The designed blade section shown in Figure 5 has been named TURBan 10/193. It can be seen in Figure 6, that the blade pressure-load, defined as the pressure difference between both sides of the blade, is almost constant from 20% to 80% of the axial chord.

3 Validation

3.1 Experimental facility

The aerodynamic characteristics of the described designed blade were validated by wind tunnel tests performed at a LNEC facility [16], using an isolated finite wing, as shown in Figure 7. The wind tunnel works in closed loop and has continuously regulated velocity up to 50 m/s and a turbulence intensity smaller than 1%. The test chamber dimensions are 1.25 × 1.0 × 3.0 m^3 and the maximum boundary layer thickness is smaller than 3 cm at the tunnel walls. The flow velocity is determined indirectly by a Betz micro-manometer connect to a Pitot-Prandtl tube.

In order to allow measuring vertical and horizontal aerodynamic forces, as well as to set appropriate flow incidence angles, α, a scaled wing model was suspended from outside of the test chamber. The force measuring devices were assembled out of six brass rings equipped with a half-bridge set of strain gauges each (Shinkoh S108-t11 with 120Ω and 8 mm length). A PEEKEL Autolog 2005 data logger controlled with dedicated software was used to collect data and the full system was previously calibrated.

3.2 Experimental results

The experimental results are presented in Figures 8, 9 and 10. For comparison, viscous flow calculations were performed using the XFoil code [10, 17], which is based upon a two-equation lagged dissipation integral method. The transition between laminar and turbulent flow is determined by an e^9-type amplification formulation. The boundary layer and the transition equations are solved simultaneously with the inviscid flow field by a global Newton method. The viscous-inviscid coupling is modelled by a wall transpiration concept where the local source strength is equal to the local mass defect gradient.

The computational Reynolds number were 3×10^5, 5×10^5 and 1×10^6. The smallest Reynolds number corresponds to the lower limit for which the XFoil was able to compute a complete polar. The experimental lift coefficient

curve compares well with the numerical values obtained with the XFoil code, except for the onset of stall, figure 8. However, the computed and the experimental drag coefficients plotted in figures 9 and 10 show significant differences, which are mainly attributed to the experimental Reynolds number being one order of magnitude lower than those used in the computations.

4 Conclusions

A pressure-load inverse design method was successfully applied to the design of a high-load blade section for application in a small wind turbine for urban environment. The pressure distribution of the designed blade shows a smooth increase of the blade pressure-load, defined as the pressure difference between the upper and the lower sides of the section, from the leading edge up to 20% of the axial chord. From 20% till 80% of the axial chord the pressure-load is almost constant and it reduces smoothly toward the trailing edge. The experimental results of the new blade section, tested as an isolated aerofoil, have confirmed the high maximum lift and a moderate drag.

Future developments will consider the application of the current design method with a viscous optimization of the thickness distribution. Due to the specification of the blade load, this methodology will reduce the drag without changing the lift.

5 Acknowledgements

This work was partially funded by Portuguese Innovation Agency, ADI, under the DEMTEC programme (Project No. 70/00201).

Nomenclature

Romans

c	=	blade chord
C_D	=	$2D/\left(\varrho V_\infty^2 c\right)$, drag coefficient
C_L	=	$2L/\left(\varrho V_\infty^2 c\right)$, lift coefficient
C_p	=	$\left(p - p_\infty\right)/\left(\varrho V_\infty^2\right)$, pressure coefficient
D	=	drag force per unit of span
i	=	$\sqrt{-1}$, unit imaginary number
L	=	lift force per unit of span
$\dot{m}$	=	mass flux
$\overline{M}_y$	=	mass average tangential momentum
p	=	static pressure
Re	=	$\varrho V_\infty c/\mu$, Reynolds number
S	=	cascade pitch
$\mathbf{U}$	=	absolute velocity
$\mathbf{W}$	=	relative velocity
$\mathbf{W}_m$	=	$\left(\mathbf{W}_1 + \mathbf{W}_2\right)/2$, mean velocity, Figure 3
w	=	complex velocity
x	=	distance along chord from leading edge
y	=	aerofoil ordinate perpendicular to chord
(x, y)	=	cartesian co-ordinate system

Greeks

α	=	angle of attack
β	=	angle of relative velocity
Γ	=	total circulation
μ	=	viscosity
ϱ	=	density
θ	=	angle of the camber line
Ω	=	control volume

Subscripts

cl	=	camber line
ps	=	blade pressure side
ss	=	blade suction side
x, y	=	axial, tangential velocity component
1, 2	=	far upstream, downstream
∞	=	far field

References

[1] Filippone A. Airfoil inverse design and optimization by means of viscous-inviscid techniques. Journal of Wind Engineering and Industrial Aerodynamics, 56(2-3):123–136, 1995.

[2] Dahl KS, Fuglsang P. Design of the wind turbine airfoil family RISØ-A-XX. Technical report, Risø-R-1024(EN), 1998.

[3] Selig MS, Maughmer MD. Multipoint inverse airfoil design method based on conformal mapping. AIAA Journal, 30(5):1162–1170, 1992.

[4] Selig MS. Multipoint inverse design of an infinite cascade of airfoils. AIAA Journal, 32(4):774–782, 1994.

[5] Obayashi S, Takanashi S. Genetic optimization of target pressure distributions for inverse design methods. AIAA Journal, 34(5):881–886, 1996.

[6] Liu GL. A new generation of inverse shape design problem in aerodynamics and aerothermoelasticity: concepts,

theory and methods. Aircraft Engineering and Aerospace Technology: An International Journal, 72(4):334–344, 2000.

[7] Borges JE, Gato LMC, Pereira RMRJ. Iterative use of a time-marching code for designing turbomachine blade rows. Computer and Fluids, 25(2):197–216, 1996.

[8] Gato LMC, Henriques JCC. Optimization of symmetrical profiles for Wells turbine rotor blades. In Proc. ASME Fluids Engng. Division Summer Meeting, number 3, pages 623–630. 1996.

[9] Kamoun B, Afungchui D, Abid M. The inverse design of the wind turbine blade sections by the singularities method. Renewable Energy, 31(13):2091–2107, 2006.

[10] Drela M. XFOIL user guide, 2006. Available at http://web.mit.edu/drela/Public/web/xfoil/.

[11] Abbott I, von Doenhoff A. Theory of Wing Sections. Dover Publications Inc., New York, 1959.

[12] Katz J, Plotkin A. Low speed aerodynamics. McGraw-Hill Publications, New York, 1991.

[13] Eça LCR. Calculation of the aerodynamic characteristics of aerofoils (in Portuguese). Master's thesis, Instituto Superior Técnico, Lisbon, 1987.

[14] Gato LMC, Henriques JCC. Optimization of symmetrical blades for Wells turbine - air turbine development and assessment for wave power plants - Contract JOU2-CT93-0333. Technical report, Instituto Superior Técnico, Lisbon, 1994.

[15] Hess JL. Review of integral-equation techniques for solving potential flow problems with emphasis on the surface-source method. Computational Methods in Applied Mechanics Engineering, 5:145–196, 1974.

[16] Borges AJ. O túnel aerodinâmico do LNEC. Technical Report Memória nº319, Laboratório Nacional de Engenharia Civil, 1986.

[17] Drela M. XFOIL: An analysis and design system for low Reynolds number airfoils. Springer-Verlag Lecture Notes in Engineering, 54, 1989.